NeuroImage 272 (2023) 120045

Contents lists available at ScienceDirect

NeuroImage

journal homepage: www.elsevier.com/locate/neuroimage

Association between sleep slow-wave activity and in-vivo estimates of myelin in healthy young men

Michele Deantoni[a,1], Marion Baillet[a,1], Gregory Hammad[a,1], Christian Berthomier[b], Mathilde Reyt[a,c], Mathieu Jaspar[d], Christelle Meyer[a], Maxime Van Egroo[e], Puneet Talwar[a], Eric Lambot[a], Sarah L. Chellappa[f], Christian Degueldre[a], André Luxen[a], Eric Salmon[a], Evelyne Balteau[a], Christophe Phillips[a], Derk-Jan Dijk[g,h], Gilles Vandewalle[a], Fabienne Collette[a,c], Pierre Maquet[a,i], Vincenzo Muto[a,*], Christina Schmidt[a,c,*]

[a] GIGA-CRC in Vivo Imaging, University of Liège, Belgium
[b] Physip, Paris, France
[c] Psychology and Neurosciences of Cognition (PsyNCog), Faculty of Psychology, Logopedics and Educational Sciences University of Liège, Belgium
[d] ARCH, Faculty of Psychology, Logopedics and Educational Sciences, University of Liège, Belgium
[e] Faculty of Health, Medicine and Life Sciences, School for Mental Health and Neuroscience, Alzheimer Centre Limburg, Maastricht University, the Netherlands
[f] Department of Nuclear Medicine, Faculty of Medicine and University Hospital Cologne, University of Cologne, Germany
[g] Sleep Research Centre, University of Surrey, Guildford, UK
[h] UK Dementia Research Institute, Care Research & Technology Centre at Imperial College London and the University of Surrey, Guildford, UK
[i] Department of Neurology, University Hospital (CHU) of Liège, Liège, Belgium

ARTICLE INFO

Keywords:
Sleep slow-wave activity
Sleep homeostasis
Myelin markers
semi-quantitative MRI

ABSTRACT

Sleep has been suggested to contribute to myelinogenesis and associated structural changes in the brain. As a principal hallmark of sleep, slow-wave activity (SWA) is homeostatically regulated but also differs between individuals. Besides its homeostatic function, SWA topography is suggested to reflect processes of brain maturation. Here, we assessed whether interindividual differences in sleep SWA and its homeostatic response to sleep manipulations are associated with in-vivo myelin estimates in a sample of healthy young men. Two hundred twenty-six participants (18–31 y.) underwent an in-lab protocol in which SWA was assessed at baseline (BAS), after sleep deprivation (high homeostatic sleep pressure, HSP) and after sleep saturation (low homeostatic sleep pressure, LSP). Early-night frontal SWA, the frontal-occipital SWA ratio, as well as the overnight exponential SWA decay were computed over sleep conditions. Semi-quantitative magnetization transfer saturation maps (MTsat), providing markers for myelin content, were acquired during a separate laboratory visit. Early-night frontal SWA was negatively associated with regional myelin estimates in the temporal portion of the inferior longitudinal fasciculus. By contrast, neither the responsiveness of SWA to sleep saturation or deprivation, its overnight dynamics, nor the frontal/occipital SWA ratio were associated with brain structural indices. Our results indicate that frontal SWA generation tracks inter-individual differences in continued structural brain re-organization during early adulthood. This stage of life is not only characterized by ongoing region-specific changes in myelin content, but also by a sharp decrease and a shift towards frontal predominance in SWA generation.

1. Introduction

Sleep is essential for everyday life quality and has been attributed to an important role in the regulation of a series of cognitive and physiological processes (Walker, 2021). Recent data relate sleep duration to structural brain changes (Tai et al., 2022), and thereby draw attention to the understanding of sleep-regulating mechanisms that may be particularly relevant for macro- and micro-structural brain integrity. As a putative marker of sleep depth (Borbely and Achermann, 1999), non-REM (NREM) sleep slow wave activity (SWA, EEG power density between 0.75–4.5 Hz during NREM sleep) represents one of the most studied electrophysiologically-derived sleep markers and mainly reveals the homeostatic regulation of sleep (Achermann and Borbély, 2003; Dijk, 2009). SWA exponentially decreases throughout nighttime sleep (Dijk et al., 1990; Dijk and Czeisler, 1995). Sleep loss evokes increased SWA during subsequent NREM sleep (Cajochen et al., 1999a;

* Corresponding authors.
E-mail addresses: vincenzo.muto@uliege.be (V. Muto), christina.schmidt@uliege.be (C. Schmidt).
[1] Equal contribution

https://doi.org/10.1016/j.neuroimage.2023.120045.
Received 4 August 2022; Received in revised form 18 January 2023; Accepted 17 March 2023
Available online 29 March 2023.

Dijk et al., 1987), while excess sleep results in an attenuation of SWA (Werth et al., 1996). Crucially, interindividual differences in SWA and its homeostatic response have been shown to be highly variable across individuals (Rusterholz et al., 2017) such that different facets of SWA regulation supposedly rely on different brain substrates or ongoing states of brain re-organization.

In healthy young adults, NREM sleep slow-wave characteristics (density and amplitude) have been associated with regional cortical gray matter thinning (Dubè et al., 2015). Furthermore, the overnight dissipation of SWA follows the overnight reduction in cortical glutamate levels, as measured by magnetic resonance spectroscopy (Volk et al., 2018). Importantly, sleep deprivation appears to alter large bilateral white matter microstructure as assessed with diffusion imaging (Voldsbekk et al., 2021). In the same vain, higher axial water diffusivity in the temporal fascicle and frontally located white matter tracts was associated with a steeper slope of sleep slow waves (Piantoni et al., 2013a) and larger corpus callosum volume has been reported to be associated with higher maximal SWA, indicating that inter-hemispheric white matter tracts contribute to cortical synchronization necessary for the generation of SWA (Buchmann et al., 2011). Notably, while the structural correlates of interindividual differences in SWA have been partially investigated in humans, the association between the homeostatic regulation of SWA and structural brain parameters has, to our knowledge, not yet been assessed. Besides its homeostatic function, more recent advances suggest that the topography of SWA reflects processes of brain maturation (e.g. Kurth et al., 2010b; LeBourgeois et al., 2019). Within this context, the ratio of frontal/occipital SWA ($SWA_{F/O}$) has been suggested to quantify the regional maturation of SWA topography in NREM sleep. SWA distribution is increased in scalp regions showing structural and behavioral maturation (Kurth et al., 2010b). $SWA_{F/O}$ has been furthermore reported to predict myelin development in children in a longitudinal study (LeBourgeois et al., 2019). Notably, investigations in children indicate that myelin is an integrative component of the propagation dynamics of slow waves across the scalp (Kurth et al., 2017), promoting the concept that regional distribution of SWA is associated with myelin connectivity in developing humans.

The brain undergoes profound changes across the lifespan (Bethlehem et al., 2022) which include both progressive and regressive cytoarchitectural events (Giorgio et al., 2010). While changes in gray matter volume have been suggested to mainly estimate mechanisms associated with cortical synaptic pruning (Terribilli et al., 2011), changes in white matter volume have been associated with myelinogenesis (Corrigan et al., 2021; Paus, 2005) and related changes in conduction velocity due to the proliferation of oligodendrocytes (Swire and Ffrench-Constant, 2018). Notably, agreement on myelin maturation dynamics and critical periods largely depends on the used methodology. While some in vivo investigations, mainly based on water fraction quantification, indicate that humans reach up to 80% of the adult white matter myelin in the very first years of life (Deoni et al., 2011), postmortem (Miller et al., 2012) and other magnetic resonance imaging (MRI)-based (Bartzokis et al., 2010) studies suggest that region-specific white matter changes are still ongoing during early adulthood. Continued postpubertal growth of myelin has indeed been suggested as unique to humans (Bartzokis et al., 2010; Miller et al., 2012). Myelination during adulthood may be reconducted to the concept of “adaptive myelination” which, compared to the “intrinsic myelination” that happens in the first stages of life, may reflect a rather selective process occurring in most active white matter tracts and thereby contributing to optimal brain wiring (Bechler et al., 2018).

Animal findings suggest a key role of sleep in promoting white matter integrity, more particularly in myelin formation (de Vivo and Bellesi, 2019). Sleep was observed to promote the proliferation of oligodendrocyte precursor cells (Bellesi et al., 2013), an essential substrate for axonal myelination (de Vivo and Bellesi, 2019). In humans, associations between electrophysiologically-derived sleep parameters and white matter integrity have been mostly derived from tract-based inference using diffusion tensor imaging (DTI) on relatively small population samples (Piantoni et al., 2013b; Voldsbekk et al., 2021). In a larger sample of healthy young adults, self-reported short sleep duration has been related to fractional anisotropy reductions in the left superior longitudinal fasciculus (Grumbach et al., 2020). Another study observed a significant association between sleep duration and fractional anisotropy in the temporal portion of the right inferior longitudinal fasciculus, in a white matter tract encompassing the orbitofrontal region as well as in the corona radiata (Khalsa et al., 2017). Finally, questionnaire-derived sleep disturbances during childhood have been associated with low white matter microstructural integrity (as assessed with fractional anisotropy) in preadolescence (Mulder et al., 2019). While DTI allows inferences on overall tract integrity and density, more recent developments in (MRI) allow for the investigation of structural properties of brain tissues at the microscopic level. In this context, quantitative MRI, also referred to as “in vivo histology”, allows to quantify physical properties of brain tissues and thereby provides a more straightforward assessment of tissue composition (Weiskopf et al., 2021). In particular, magnetization transfer saturation (MTsat) maps have been previously used as reliable MRI-derived estimates of macromolecular content, including myelin (Campbell et al., 2018). Moreover, compared to classical anatomical imaging, MTsat improves gray/white matter contrast which makes this technique also suitable for classic volumetric analyses such as voxel-based morphometry (VBM) (Callaghan et al., 2014; Hagiwara et al., 2018).

Here, we first aimed at characterizing the individual’s characteristics of SWA generation and its homeostatic response to sleep-wake history manipulation. In addition, the ratio between frontal and occipital SWA was computed as a marker of brain maturation. In a next step, we aimed at assessing whether these characteristics are associated with regional myelin estimates during early adulthood. To do so, a cohort of 226 healthy young men underwent a 6-day in-lab protocol during which prior sleep-wake history was experimentally manipulated to assess homeostatic responses in SWA. During a separate visit, the same individuals underwent brain structural imaging.

2. Methods

The research project was approved by the Ethics Committee of the Faculty of Medicine at the University of Liège (Belgium) and was performed in accordance with the Declaration of Helsinki. All participants signed informed consent before taking part in the study and received financial compensation.

2.1. Participants

A total of 364 young healthy men were initially recruited as part of a larger project assessing the genetic background of sleep regulation (see also Berthomier et al., 2020; Muto et al., 2021). Within that context, a homogeneous sample with respect to demographic variables (age [18–31], gender [male], ethnicity [Caucasian]) and health status was recruited. Exclusion criteria were as follows: body mass index (BMI) > 27; presence of psychiatric history or severe brain injury; addiction; chronic medication affecting the central nervous system; smoking, excessive alcohol (> 14 units/week) or caffeine (> 3 cups/day) intake; shift work in the past year; trans-meridian travels in the past 3 months; presence of moderate to severe subjective depression as measured by the Beck Depression Inventory (score > 19; Beck et al., 1988) and poor sleep quality as assessed by the Pittsburgh Sleep Quality Index (PSQI score > 7; Buysse et al., 1989). Participants with sleep apnea (apnea-hypopnea index > 15/h; Iber et al., 2007) or periodic limb movements (>15/h) were excluded based on an in-lab screening night of polysomnography.

Out of that sample, artefact-free sleep electrophysiological recordings were available for 337 participants out of which 236 magnetic resonance imaging (MRI) acquisitions were available for the creation of MT

Table 1
Demographic and sleep characteristics of participants. Sleep quality was assessed by the Pittsburgh Sleep Quality Index (PSQI; Buysse et al., 1989). IQ was calculated from the Raven Matrices (John and Raven, 2003). Chronotype was assessed by the Morningness-Eveningness Questionnaire (MEQ; Horne and Ostberg, 1976). Sleep timing and duration were extracted from polysomnography recordings during the baseline night (see below). SD: standard deviation.

Sample size (N)	$N = 236$	
Sex	Men	
Ethnicity	Caucasian	
	Mean (± SD)	**Min-Max**
Age (years)	22.23 ± 2.72	18 - 31
BMI (kg^*m^{-2})	22.19 ± 2.32	17.83 – 27.75
Height (cm)	180.69 ± 7.14	163 - 205
IQ (Raven Sum)	54.84 ± 4.18	31 - 60
Sleep Quality (PSQI – total score)	3.45 ± 1.71	1 - 9
Chronotype (MEQ)	48.37 ± 12.71	1 - 74
Sleep duration during baseline night (min)	453.60 ± 40.74	318.5 - 561
Sleep timing (min)	23:44:45 ± 1:23:02	21:25:30 – 02:51:17

saturation (MTsat) maps. Demographic characteristics are summarized in Table 1.

2.2. Experimental protocol

To assess the impact of sleep-wake history on sleep parameters, participants underwent a 6-day in-lab protocol as depicted in Fig. 1. Before entering the laboratory, they were instructed to follow a regular schedule according to their habitual sleep-wake timing (+/−30 min for the first 2 weeks; +/- 15 min for the last week). Actimeters (Actiwatch 4, CamNtech, Cambridge, UK) were worn on the non-dominant arm for three weeks preceding the in-lab protocol. The first 2-weeks of recording were used to assess the individual's usual bedtimes (nighttime rest timing and duration). Each recording was visually inspected to derive daily bedtimes. The latter were then confronted with the information of sleep diaries to extract the individual's sleep-wake-time schedule to be followed during the third week. This schedule was also followed during the laboratory session. Furthermore, actimetry recordings served to exclude participants who did not comply with the assigned schedule during the last week preceding the in-lab assessment. This procedure was performed to ensure sufficient sleep and stable circadian entrainment to the selected regime before laboratory entrance. Participants who could not avoid napping were excluded after visual inspection of the actigraphy recordings (periods of reduced daily activity). A negative result on a urine drug screening test was required at study entrance (10 Multipanel test, SureScreen Diagnostic Ltd, UK). Participants entered the sleep laboratory 3.5 h before scheduled bedtime. They then underwent complete polysomnography (PSG) recording to screen for sleep-related disorders (screening night) according to their habitual sleep-wake schedule. On the morning of day 2, participants left the laboratory with the instruction not to nap, retrospectively visually checked by actimetry. They came back to the laboratory at the end of day 2 (3.5 h before scheduled lights-off) and completed a baseline night (BAS), the duration and timing of which were individually adapted to their habitual sleep-wake schedule. On the evening of day 3, participants underwent a 12-h sleep extension night (EXT, centered on the habitual sleep mid-point time), followed the next day by a 4-h afternoon nap (NAP; centered on +1 h after the mid-point between the usual morning wake-up time and evening sleep time). Adding a 4 h day-time sleep opportunity to the nighttime sleep extension was intended to keep sleep pressure at its lowest level, considering that sleep pressure accumulates with time spent awake and that there may be interindividual differences in the ability to sleep during the sleep extension night. The EXT and NAP sleep opportunities were thus part of the protocol, but not explicitly analyzed as they were included with the main aim to achieve maximal sleep satiation before assessing sleep during the following night (LSP for low sleep pressure condition). The latter consisted of an 8-h sleep opportunity centered on habitual sleep mid-point. On days 5 and 6, participants underwent a 40-h sleep deprivation protocol under constant routine (CR) conditions (dim light < 5 lux; room temperature = 19° ± 1; ~ 60% humidity; semi-recumbent position; regular isocaloric food intake) before initiating a 12-h recovery night (HSP, for high sleep pressure condition) at the habitual sleep time until 4-h after the habitual wake time. At regular intervals during scheduled wakefulness, participants had to complete subjective

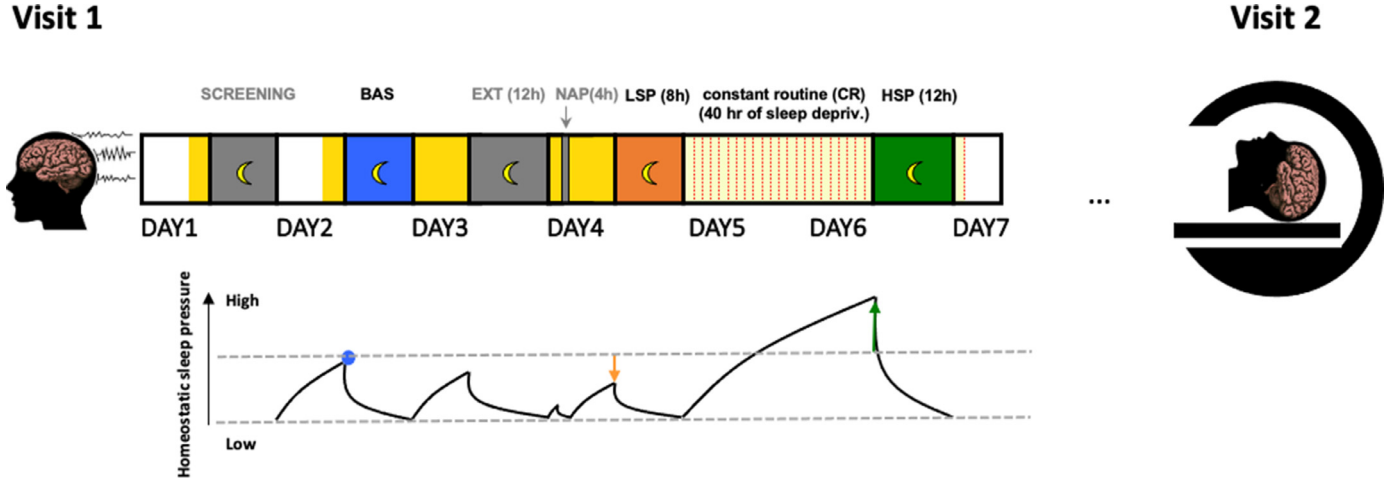

Fig. 1. Experimental protocol.
On Day 1, participants first entered the sleep laboratory for a screening night. They then left the laboratory on the morning of Day 2 and came back at the end of the day to complete a baseline night (BAS, blue). After the baseline night, participants underwent a 12-h sleep extension night (EXT, Day 3–4), and a 4-h afternoon nap opportunity (NAP) on Day 4, followed by an 8-h sleep opportunity (LSP, orange; Day 4–5). Finally, participants underwent a 40-h constant routine sleep deprivation protocol (including regular collection of saliva samples, sleepiness, vigilance and cognitive assessments; red bars), starting on the morning of Day 5. Day 6 ended with a 12-h recovery night (HSP, green). Light exposure levels were set to 0 lux during sleep opportunities, < 1000 lux during the laboratory stays Day 1-Day 4 (yellow shaded boxes) and to < 5 lux during the constant routine sleep deprivation (light yellow shaded box). The order of the protocol was the same for each participant. After successful completion of the in-lab protocol, participants came back to the laboratory on average 3 weeks later for the structural MRI session. Varying levels of homeostatic sleep pressure levels across the protocol are schematized at the bottom of the protocol: baseline levels during the BAS: blue dot; reduced levels in response to sleep saturation (probed during LSP): orange arrow; increased levels in response to sleep deprivation (probed during the HSP): green arrow.

sleepiness scales, mood ratings and to perform a cognitive test battery and Karolinska Drowsiness tests (KDT, Åkerstedt and Gillberg, 1990; Dinges and Powell, 1985; Kirchner, 1958; Robertson et al., 1997). They were also asked to provide saliva samples for melatonin assessment. In between these assessments, participants could read but mainly watched pre-selected videos on the laboratory computer (the screen was dimmed to not exceed 5 lux of light exposure). Social interaction was restricted to communications with study helpers. Throughout the entire laboratory stay, participants were in individual and soundproof rooms, and under electroencephalographic (EEG) monitoring.

2.3. EEG acquisition and analyses

EEG data were acquired using V-Amp amplifiers (Brain Products®, Gilching, Germany) and digitized at a sampling rate of 500 Hz. For the screening night, the montage included 5 EEG channels (Fz, Cz, C3, Pz, Oz) as well as 2 electromyography (EMG) electrodes. Leg movements as well as thoracic movement nasal flow and oximetry were also recorded. The electrode montage of the experimental nights consisted of 10 derivations (F3, Fz, F4, C3, Cz, C4, Pz, O1, O2, and A1; referenced online to the right mastoid), as well as 2 electrooculogram (EOG), 2 electromyogram (EMG), and 2 electrocardiography (ECG) electrodes. EEG data were re-referenced offline to averaged mastoids. Sleep scoring was performed automatically according to the 2017 American Academy of Sleep Medicine criteria (version 2.4; Iber et al., 2007), by using a validated algorithm (ASEEGA, PHYSIP, Paris, France; Berthomier et al., 2020).

Spectral power was computed using a fast Fourier transform after convolution of the signal with Hamming windows. A spike-cleaning routine was further applied: for each epoch n, the ratio between the EEG power of the epoch n and the mean EEG power of epochs $n-1$ and $n+1$, was computed. If the ratio exceeded a threshold of 10, the epoch was discarded from the analysis. SWA was calculated on artefact-free NREM (N1, N2 or N3) epochs as the mean power in the slow-wave frequency band ([0.7–4.0] Hz) and over successive 2-h bins starting at the first epoch of N2, for each sleep condition separately.

The frontal derivation was chosen as a main outcome since homeostatic responses in SWA have been reported to be most prominent in frontal regions (Cajochen et al., 1999b; Finelli et al., 2001; Lazar et al., 2015). Normalized frontal SWA (expressed as a proportion of power over the entire frequency range [0.7–50 Hz]) in the first 2-h bin of each sleep episode was extracted (SWA_{0-2h}). Furthermore, overnight SWA dissipation time (τ) was computed by fitting an exponential model ($SWA_0 \times \exp(\frac{-\tau}{t}) + offset$) to the absolute SWA values obtained in each 2-h bin. Combined, these two outcomes suitably summarize the classically observed wake-dependent increase in SWA levels as well as its overnight dynamics. Additionally, frontal SWA responsiveness to disproportionally low (after sleep extension) and high (after sleep deprivation) sleep pressure conditions was computed as the proportional change of normalized SWA_{0-2h} from the BAS to the LSP (SWA_{0-2h}_ratioLSP) and the HSP (SWA_{0-2h}_ratioHSP) nights over the frontal derivation, respectively: $\frac{\text{SWA0–2h } (HSP \text{ or } LSP) - \text{SWA0–2h } BAS}{\text{SWA0–2h } BAS}$. Finally, the frontal/occipital ratio ($SWA_{F/O}$) was computed by dividing the mean SWA_{0-2h} from the frontal derivations (F3, F4) by the mean SWA_{0-2h} from the occipital derivations (O1, O2) in each individual (Kurth et al., 2010b; LeBourgeois et al., 2019). Data of sufficient quality regarding this index was available for 229 participants out of the 236 initially included.

2.4. MRI acquisition and pre-processing

On average 3 weeks after completion of the sleep study protocol, participants were examined on a 3T MR system. MRI data were acquired on a 3T head-only MRI scanner (Magnetom Allegra, Siemens Medical Solutions, Erlangen, Germany) for 212 participants. MRI data for the remaining 24 participants were acquired on a 3T whole-body MRI scanner (Magnetom Prisma, Siemens Medical Solutions, Erlangen, Germany), due to scanner replacement. The MR acquisition included a whole-brain quantitative multiparameter protocol (MPM) as described in (Weiskopf et al., 2013a) and (Tabelow et al., 2019).

The MPM protocol has been gradually optimized and validated for multi-centric acquisitions (Weiskopf et al., 2013b). It consists of three co-localized series of 3D multi-echo fast low angle shot (FLASH) acquisitions at $1 \times 1 \times 1$ mm^3 resolution and two additional calibration sequences to correct for inhomogeneities in the radio frequency (RF) transmit field (Lutti et al., 2012). The FLASH data sets were acquired with predominantly proton density (PD), longitudinal relaxation time (T1), and magnetization transfer (MT) weighting, in the following referred to as PDw, T1w and MTw echoes. Volumes were acquired in 176 sagittal slices using a 256×224 voxel matrix. Supplemental details of acquisition parameters used for this study are available in Table S1.

The multi-parametric echo (PDw, T1w, and MTw) images were auto-reoriented to approximately match the MNI space and MTsat, PD, R1 and R2* maps were created using the hMRI toolbox (v0.1.2-beta, Tabelow et al., 2019, see also: http://hmri.info) within the SPM12 environment (Statistical Parametric Mapping, Wellcome centre for Human Neuroimaging, London, UK, http://www.fil.ion.ucl.ac.uk/spm, University College London, revision 12.4). Here, we focused on the exploration of MTsat maps. MTsat is related to the exchange of magnetization between mobile water protons and protons that are bound to macromolecules such as myelin. MTsat values have been closely related to myelin content as shown in postmortem studies (Schmierer et al., 2004). Contrary to the commonly used MT ratio (percentage reduction in steady-state signal), the MTsat map explicitly accounts for spatially varying T1 relaxation time and flip angles (Helms et al., 2021). The map creation module includes the determination of B1 transmit bias field maps for bias correction. For this dataset, two different methods were used, the EPI spin-echo (EPI, $n = 99$) (Lutti et al., 2012) and Actual Flip-angle Imaging (AFI, $n = 137$) method (Yarnykh, 2007).

2.5. Voxel-based morphometry and quantification

Voxel-based morphometry (VBM) was used to estimate local gray and white matter volumes. To do so, MTsat maps were first segmented into gray matter, white matter, and cerebrospinal fluid posterior probability maps using the hMRI toolbox (Tabelow et al., 2019). Segmented gray- and white matter tissue maps were then non-linearly warped to a study-specific template using the DARTEL method (Ashburner, 2007), modulated, and finally smoothed with an isotropic Gaussian smoothing kernel of 6 mm full width at half maximum (FWHM). VBM analysis was carried out in the gray matter compartment using the CAT12 software (v12.8) (Farokhian et al., 2017). Total intracranial volume (TIV) was computed as the sum of gray matter, white matter and cerebrospinal fluid volumes using the "Get TIV" function of the CAT12 software (Gaser and Dahnke, 2016).

Semi-quantitative MTsat-derived myelin markers were estimated using voxel-based quantitative analyses (VBQ). As for VBM, gray matter and white matter probability maps, derived from the segmentation of the MTsat maps, were used to create a study-specific DARTEL template (Ashburner, 2007). MPM maps were then non-linearly and linearly warped to the MNI space using the subject-specific diffeomorphic estimates from the DARTEL procedure and an affine transformation, respectively. MPM maps were finally smoothed with a kernel of 6 mm using a tissue-specific weighting which accounts for partial volume distribution of white and gray matter tissue in each voxel (Draganski et al., 2011).

2.6. Statistical analyses

Normalized SWA in the first 2-h bin (SWA_{0-2h}) (Achermann and Borbély, 1990) and τ dissipation time ($SWA\tau$) at the frontal derivation were compared across conditions by using repeated measures ANOVAs, including BAS, LSP and HSP nights as repeated factors and subjects as

random factor. Tukey pairwise *t*-tests were performed for post-hoc comparisons. Linear regression models were further deployed to explore the association between age and SWA markers. Statistics were performed using the Python statsmodel toolbox (version 3.7) (Seabold and Perktold, 2010). Significance was based on a two-tailed *p*-value < 0.05.

For the brain imaging analyses, we carried out multiple linear regression models embedded in the general linear model framework of SPM12. The first statistical model included normalized frontal SWA over the first two hours of the baseline night ($SWA_{0–2h}$_BAS), its responsiveness to disproportionally low ($SWA_{0–2h}$_ratioLSP) and high ($SWA_{0–2h}$_ratioHSP) sleep pressure conditions and overnight frontal-derived SWA dissipation dynamics (SWAτ_BAS). A separate model was computed for $SWA_{F/O}$. TIV and age were included as covariates in both models. Age was included to regress out the effect of the latter on the association between sleep and brain metrics, but also to assess age-related changes in brain metrics, as such. Differences in scanning environment and sequences (EPI-Prisma, AFI-Allegra, EPI-Allegra, see supplemental information) were embedded using a 3-level full factorial design. Gray and white matter masks were extracted from the hMRI toolbox and used for statistical analyses. T-contrasts were computed to assess the relationship between each regressor of interest (age, SWA characteristics) and gray matter volume fraction, as well as gray and white matter MTsat values. Inferences were performed using whole-brain family-wise corrected *p*-values with a threshold set at $p < 0.05$, at the cluster level (cluster forming threshold at $p < 0.0001$ uncorrected rather than $p < 0.001$, in order to favor parsimony in the construction of the model; k = number of voxels in the cluster). For anatomical labeling, the Harvard-Oxford Cortical structural atlas for gray matter (Frazier et al., 2005), and the John Hopkins University (JHU) white matter tractography atlas (Ling and Rumpel, 2006) were used.

For VBQ, a sensitivity analysis was performed on a reduced sample of individuals for which the MPM protocol was acquired in the same scanner and using the same sequence (n = 137, AFI-Allegra) to reproduce the analysis without potential confounding effects of the scanning environment (Weiskopf et al., 2013a).

3. Results

3.1. Effect of sleep condition on SWA parameters

Overnight time courses of absolute frontal SWA according to sleep condition are depicted in Fig. 2A. Normalized $SWA_{0–2h}$ values, as

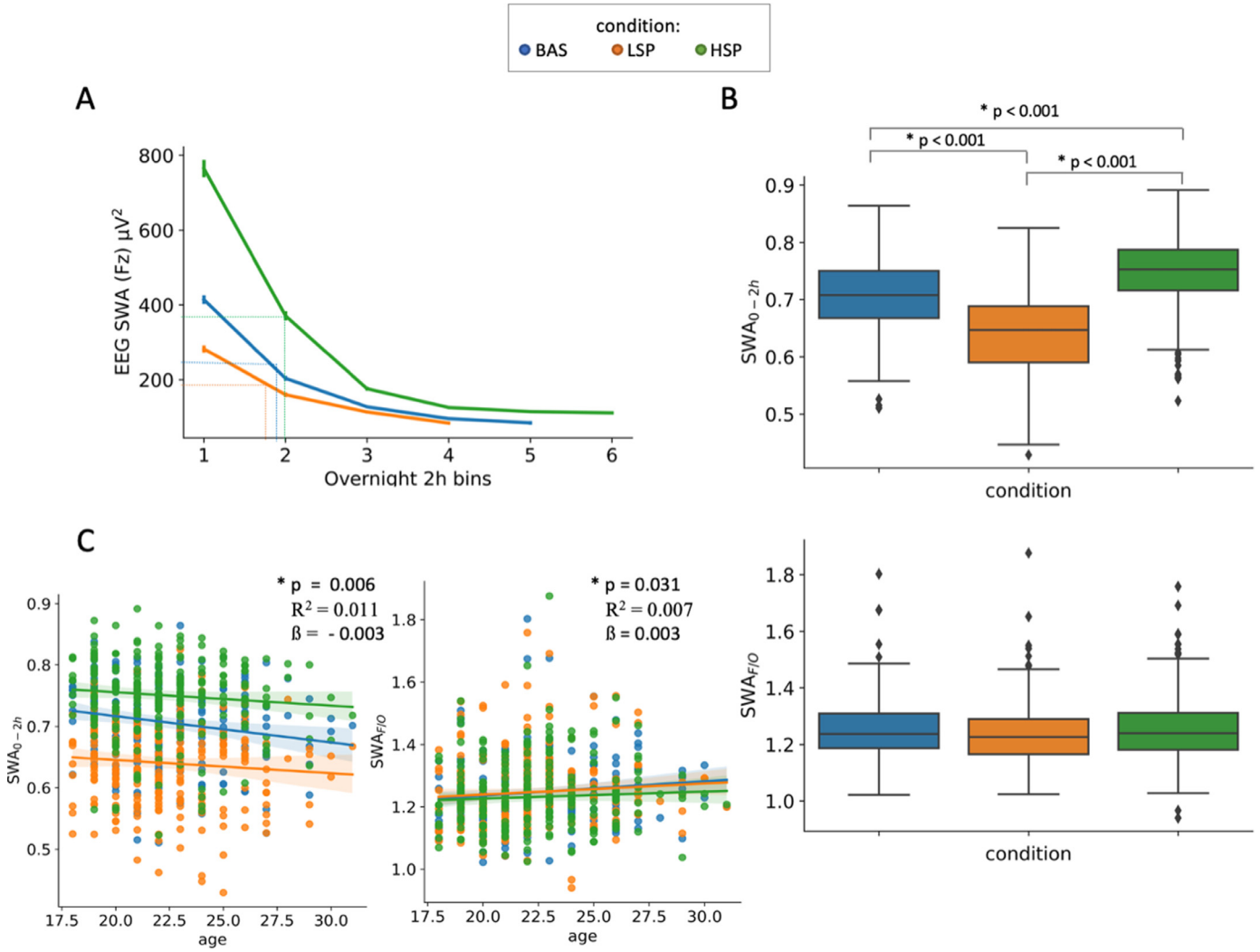

Fig. 2. (A) Overnight time course of absolute SWA (0.7–4.0 Hz, mean ± standard error of the mean) computed over the frontal derivation during the baseline (BAS, blue), the low sleep pressure (LSP, orange) and the high sleep pressure (HSP, green) conditions. The dotted line highlights the time at which SWA decreases at half of the maximum level (dissipation time, SWAτ). (B) Normalized frontal SWA levels over the first 2 h of sleep ($SWA_{0–2h}$; upper panel) and the frontal/occipital SWA ratio ($SWA_{F/O;}$ lower panel) by sleep condition. (C) Association between age (derived from the year of birth) and normalized frontal $SWA_{0–2h}$ (left panel) and the frontal/occipital SWA ratio ($SWA_{F/O;}$ right panel) during the baseline (blue), the LSP (orange) and HSP (green) nights, respectively.

depicted in Fig. 2B, were used for statistical analyses. A significant main effect of sleep condition (BAS, HSP, LSP) was observed for normalized frontal $SWA_{0–2h}$ ($F(2, 470) = 538.36$, $p < 0.001$; Fig. 2B) and overnight SWA dissipation time ($SWA\tau$; $F(2, 470) = 4.53$, $p < 0.05$). Post-hoc contrasts revealed that $SWA_{0–2h}$ and $SWA\tau$ statistically differed between all sleep conditions of interest (HSP > BAS > LSP for $SWA_{0–2h}$ and LSP>BAS/HSP for $SWA\tau$; all p-values < 0.001, see Table S1 for mean ± SD values of SWA parameters by sleep condition). For $SWA_{F/O}$, while the main effect of sleep condition reached significance, ($SWA_{F/O}$, $F(2, 456) = 3.511$, $p < 0.05$, Fig. 2B), post-hoc contrasts did not detect significant differences between any of the sleep conditions compared separately (all p-values > 0.05).

3.2. Sleep parameters and brain structural indices: association with chronological age

For the sleep SWA measures, we observed that, within the context of the relatively narrow age range of our sample, frontal $SWA_{0–2h}$ was significantly negatively associated with age across all three sleep conditions of interest (main effect of age: $F(1706) = 7.650$, $p < 0.05$, $R^2 = 0.011$; Fig. 2C). $SWA_{0–2h}$_ratioHSP was positively associated with age ($F(1, 706) = 11.37$, $p = 0.001$; $R^2 = 0.016$). Likewise, $SWA_{F/O}$ was positively associated with age in all sleep conditions ($F(1, 685) = 4.679$, $p < 0.05$, $R^2 = 0.007$, Fig. 2C).

For brain structural indices, we observed that gray matter volume decreased significantly with age in a set of regions including the bilateral superior frontal gyrus, postcentral gyrus, as well as parietal and superior-temporal regions (Fig. S1, Table S2). No significant associations were observed between age and gray- and white matter MTsat-derived myelin estimates (all $pFWE_{corr} > 0.05$).

3.3. Association between brain structural indices and sleep SWA parameters

No significant associations were observed between sleep SWA parameters and gray matter volume. However, whole-brain voxel-wise analyses revealed that frontal $SWA_{0–2h}$_BAS was negatively associated with white matter MTsat values in a cluster encompassing the right temporal portion of the inferior longitudinal fasciculus ($k = 2327$; $pFWE_{corr} = 0.001$; peak voxel coordinates: $x = 40$ $y = 3$ $z = -29$; Fig. 3A, dark blue). A follow-up analysis on a reduced sample of 137 participants scanned in the same environment corroborated the association

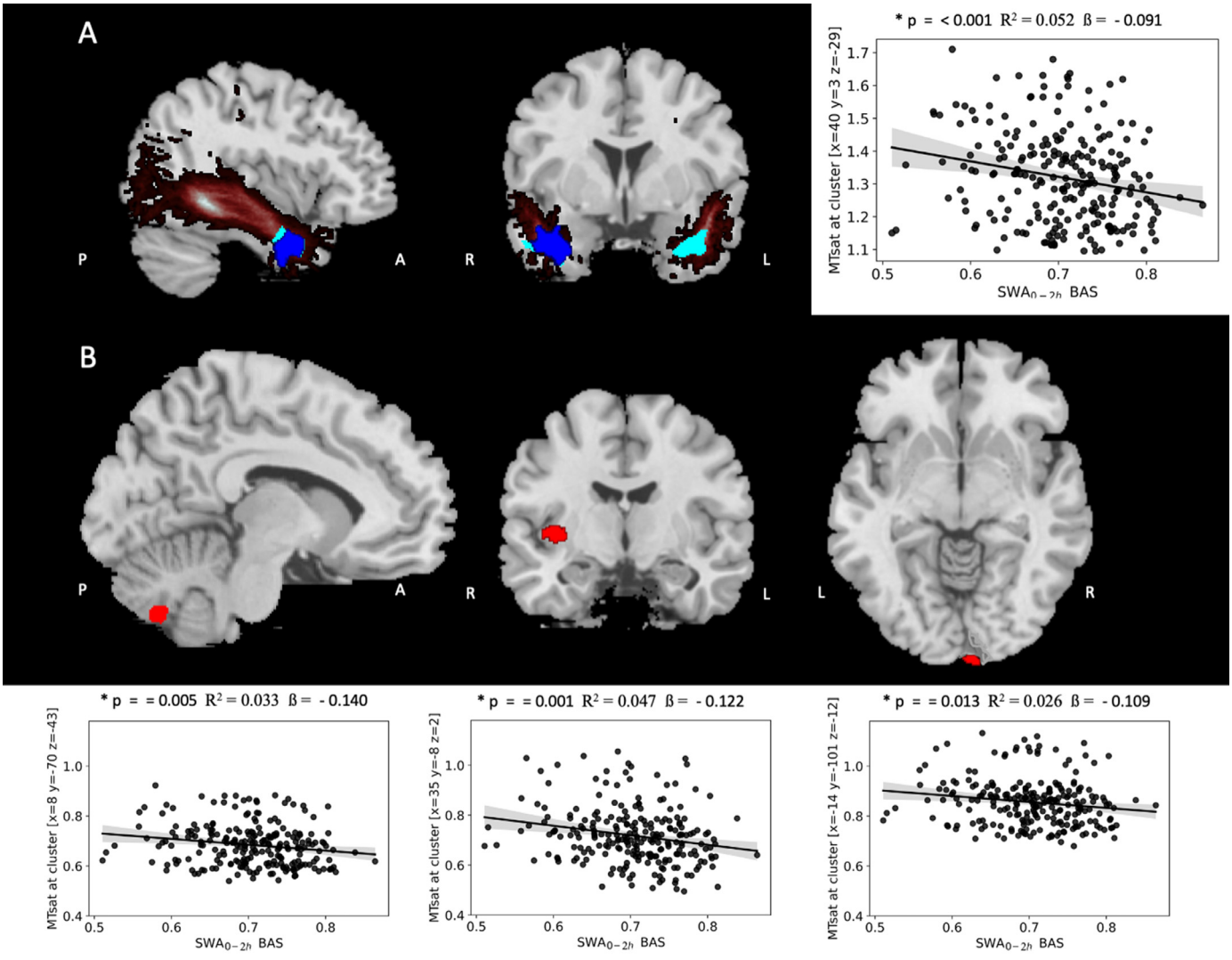

Fig. 3. (A) Regions and corresponding regression plot depicting the negative association between normalized $SWA_{0–2h}$ (extracted from Fz) during baseline sleep and white matter MTsat (dark blue). The light blue blobs reflect the same analysis performed on a reduced sample of 137 participants for which the MPM protocol was acquired in the same scanning environment. The probabilistic tracts highlighted in copper color correspond to the Inferior Longitudinal Fasciculus (ILF). (B) Regions and corresponding regression plots depicting the negative association between gray matter MTsat values and $SWA_{0–2h}$_BAS (red). $pFWE_{corr}$ at the cluster level < 0.05.

reported between SWA_{0-2h}_BAS and white matter MTsat values over the whole sample, while further extending the association in the left temporal portion ($k = 1436$, $pFWE_{corr} = 0.012$, peak voxel coordinates: $x = -34$ $y = -2$ $z = -31$) as well as in the right occipital portion ($k = 754$, $pFWE_{corr} = 0.043$, peak voxel coordinates: $x = -58$ $y = -28$ $z = 10$) of the inferior longitudinal fasciculus (Fig. 3a, light blue). For gray matter, MTsat values were significantly negatively associated with SWA_{0-2h}_BAS in the occipital lobe ($k = 704$; $pFWE_{corr} = 0.006$; peak voxel coordinates: $x = -14$ $y = -101$ $z = -12$), the cerebellum ($k = 734$; $pFWE_{corr} = 0.005$; peak voxel coordinates: $x = 8$ $y = -70$ $z = -43$) and the temporal lobe, extending into the insula ($k = 754$; $pFWE_{corr} = 0.029$; peak voxel coordinates: $x = 35$ $y = -8$ $z = 2$, Fig. 3B). No significant associations were observed between MTsat and the homeostatic responses to sleep saturation (SWA_{0-2h}_ratio_LSP) and sleep deprivation (SWA_{0-2h}_ratio_HSP), respectively, nor with SWAτ_BAS in both gray and white matter (all $pFWE_{corr} > 0.05$). Finally, when performing the same analysis between $SWA_{F/O}$_BAS and white/gray matter MTsat values, no significant associations were observed (all $pFWE_{corr} > 0.05$).

4. Discussion

In this study, we assessed whether sleep SWA,its intra- and inter-night dynamics, as well as its anteroposterior distribution are associated with myelin estimates in healthy young men. We observed that frontal SWA generation was significantly modulated by sleep-wake history and age, while the frontal/occipital SWA ratio was positively associated with age but appeared to not significantly differ between sleep conditions considered separately. The frontal/occipital SWA ratio has been assumed to mainly reflect processes of brain maturation, while frontal SWA_{0-2h} may reflect the overall ability to generate slow waves, both in an age- and sleep-wake-history-dependent manner. Within this context, we observed a negative association between early-night frontal SWA and myelin estimates which was circumscribed to the late-myelinating temporal portion of the inferior longitudinal fasciculus. No association was observed with myelin estimates and wake-dependent SWA modulation, its overnight dynamics nor with the frontal/occipital SWA ratio. These data thus suggest that frontal SWA is a potential sleep trait that is rather specifically associated with regional myelination in healthy young men. Importantly, these results were observed while correcting for age (and in the absence of a significant association between age and myelin markers), thereby suggesting that frontal SWA may be sensitive to track myelin changes in healthy young men.

4.1. Slow-wave activity & sleep homeostasis during early adulthood

SWA has been widely used as an electrophysiological correlate for sleep depth (Borbely and Achermann, 1999) and mainly reveals the homeostatic regulation of sleep (Achermann and Borbély, 2003; Borbély, 1982; Dijk, 2009). Topographical analyses demonstrated that the sleep-dependent modulation of slow wave characteristics was most prominent in frontal derivations whereas the circadian effect was similar to or greater than the sleep-dependent modulation over the central and posterior brain regions (Lazar et al., 2015). Here, as expected, we observed that frontal SWA_{0-2h} was lowest in response to sleep saturation and highest after a 40-h total sleep deprivation, compared to baseline sleep. Similarly, the overnight SWA dissipation rate depended on the sleep context, with faster decline rates in response to sleep deprivation and the lowest rates following the night after sleep saturation.

We further observed that increasing age was associated with reduced frontal SWA and an increased frontal/occipital SWA ratio in all sleep conditions, and this even within the context of the narrow age range considered in our study. This observation is in line with previous reports indicating that sleep SWA sharply declines across puberty (Kurth et al., 2010a) and is followed by a smaller decrease thereafter (Gaudreau et al., 2001). Additionally, an increased frontal over occipital predominance in NREM SWA has been observed during development (Kurth et al., 2010b), as reflected by the $SWA_{F/O}$ marker in our study. Besides, we observed that the overnight SWA dissipation rate (SWAτ) depended on the sleep context, with faster decline rates in response to sleep deprivation and lowest rates following the night after sleep saturation. In addition, we found a positive association between SWA dissipation time and age, suggesting longer homeostatic sleep pressure dissipation times with increasing age during early adulthood. This finding might appear unexpected at first glance but can be set in the context of studies in adolescents where it was observed that sleep deprivation resulted in a larger increase in low-frequency power in the older compared with the younger participants, suggesting that the younger individuals more quickly reach maximal capacity for generating low-frequency activity (Tarokh et al., 2010). In parallel, it has to be noted that the response to sleep deprivation (expressed as percentage change from baseline) depends on both, dissipation time and SWA levels during baseline sleep, putatively underlined by different sleep pressure levels at study entry and thereby affecting the reported percentual change.

4.2. Slow-wave activity, sleep homeostasis & myelin content during early adulthood

The association between SWA and regional myelin estimates was observed for SWA generation during baseline sleep (SWA_{0-2h}_BAS), but not for indices describing its homeostatic response to sleep saturation and deprivation (SWA_{0-2h}_ratioLSP, SWA_{0-2h}_ratioHSP), nor its overnight dynamics (SWAτ), or the frontal/occipital ratio ($SWA_{F/O}$). This suggests that not all characteristics of SWA regulation are equally associated with brain microstructural integrity during early adulthood. As mentioned above, $SWA_{F/O}$ has been suggested to predominantly reflect a maturational NREM sleep marker (Kurth et al., 2010b). The latter appeared not to be significantly associated with myelin markers in our cohort of young men. SWA generation (estimated here by SWA_{0-2h}_BAS) and its modulation by sleep context (reflected here by SWA_{0-2h}_ratioLSP, SWA_{0-2h}_ratioHSP) have been globally pinned down to sleep depth and homeostatic sleep regulation (Borbely and Achermann, 1999). In rodents, slow-wave sleep homeostasis has been shown to be under genetic control such that wake-dependent slow-wave sleep need appears genetically driven, contrary to the rate at which slow-wave sleep need decreases overnight (Franken et al., 2001). Likewise, in humans the time constants of homeostatic build-up and dissipation of SWA have been shown to vary independently among human individuals (Rusterholz et al., 2017), indicating different traits. Accordingly, our results suggest that, during early adulthood, the trait-like expression of SWA (SWA_{0-2h}) is associated with myelin estimates.

Despite the suggested role of sleep in myelin genesis (Bellesi et al., 2013), the association between SWA and white matter integrity is not very well established in young adults. At the macrostructural level, one study observed that the volume of the anterior part of the corpus callosum was positively associated with maximal SWA over nighttime (Buchmann et al., 2011). In addition, a steeper rising slope of sleep slow-waves, but not slow-wave density, has been associated with higher DTI-derived axial diffusivity – mainly reflecting axonal integrity (Song et al., 2002) - in the temporal fascicle and frontally located white matter tracts in healthy young men (Piantoni et al., 2013a). However, another study failed to replicate such association in healthy young adults but found that greater white matter damage in brain-injured patients over frontal and temporal brain regions was positively associated with slow-wave amplitude and slope (Sanchez et al., 2019).

Complementary to volumetric or diffusion-weighted imaging techniques, MTsat imaging quantifies the exchange of protons between bound and free water, the intensity of which relates to macromolecular concentration. MTsat values have been associated with ex-vivo measured processes of de-myelination and re-myelination (Turati et al., 2015). From a functional point of view, while the MTsat signal in the white matter has been related to the myelination of long-reach fibres, MTsat in the cortical gray matter has been suggested

to be linked to the myelination of short-distance cortical fibers (Corrigan et al., 2021) which might jointly contribute to SWA generation (Tononi and Cirelli, 2014). Here, we also observed associations between $SWA_{0–2h}$_BAS with gray matter myelin content. Myelination in gray and white matter not only differs in the type of fibers involved (short vs long) but also in their biological function. Myelination in white matter grants conduction velocity and is needed to improve the connectivity of distal regions (Corrigan et al., 2021) thereby potentially supporting long-range measures of EEG coherence and travelling waves (Kurth et al., 2017). Concomitantly, in gray matter, myelin has been suggested to serve as metabolic assistance for providing energy supply (Timmler and Simons, 2019) and to rather support local neuronal connectivity. Moreover, one function of gray matter myelin could be the prevention of aberrant axonal sprouting and synapse formation, also partly explaining why more plastic cortical regions take more time to be myelinated: only when the neural remodeling is terminated, myelination may put a seal on neuronal plasticity to consolidate the acquired skills (Timmler and Simons, 2019).

While the age-related changes in SWA dynamics co-occur with both ongoing progressive (myelination) and regressive (synaptic pruning) cellular events (Miller et al., 2012; Petanjek et al., 2011), the mechanisms that link synaptic pruning, SWA generation and fiber myelination are not yet explored. It may be assumed that pruning and myelination reflect two stages of a biophysical cascade that switch from a brain rich in synapses and SWA (Vyazovskiy et al., 2007) to a brain that is optimized through distal myelin, more weighted on long-range connectivity and associated slow waves propagation (Tarokh et al., 2010).

4.3. Regional specificity of the association between SWA markers and myelin estimates

Besides differences in their overall developmental chronicity, regional differences in both gray (Bethlehem et al., 2022; Gogtay and Thompson, 2010; Shaw et al., 2008) and white (Bartzokis et al., 2001) matter volume trajectories have been identified such that peak volumes are observed earlier in the occipital lobe and later in the frontal and temporal lobe. For gray matter, reduced early-night SWA was associated with increased myelin estimates in cerebellar, occipital and temporal regions. The regions serve different functional outcomes and gray matter myelin development has been shown to follow different trajectories in these regions during adolescence (Corrigan et al., 2021). This makes it challenging to draw a unifying conclusion about regional specificity unless to observe that all the regions show plasticity in the adult brain (Castaldi et al., 2020; Ohtsuki et al., 2020; Valk et al., 2017). For white matter, reduced early-night SWA was associated with an increase in white matter myelin estimates circumscribed to the temporal portion of the inferior longitudinal fasciculus (ILF). The ILF represents an associative bundle that mainly connects the temporal lobe with parieto-occipital cortices. Notably, the temporal lobe is among the last maturating regions such that, throughout adulthood, myelin content appears to peak only around age 45 on average (Armstrong et al., 2004; Bartzokis et al., 2001; Mehta et al., 1995). The temporal portion of the ILF is amongst the latest myelinating tracts (Lynch et al., 2020) and the temporal pole as such reflects a higher-order associative cortex that classically subserves multi-sensory integration (Ohki et al., 2016).

5. Limitations and perspectives

Our sample of participants was recruited in the context of a project that aimed to assess the genetic background of sleep regulation (e.g. Muto et al., 2021) and is thus only composed of men, mainly university students. Women have been shown to present higher sleep SWA than men, and this difference seems to be present in adults of various ages (Carrier et al., 2001; Dijk, 2006; Dijk et al., 1989). The present work aimed to assess the associations between slow-wave sleep and its homeostatic regulation on brain integrity in a homogeneous sample. Extending these findings to a more population-representative dataset is a needed future avenue.

Another possible limitation is the presence of two different scanning environments and acquisition protocols, even if the quantitative approach should alleviate potential inter-scanner biases. Notably, our follow-up analysis on a subsample of individuals scanned in the same scanning environment confirmed our findings over the entire sample.

Furthermore, a longitudinal assessment of myelin markers and sleep SWA signatures would allow further disentangle respective impact or specific associations between sleep-state, sleep-trait and sleep-developmental characteristics of SWA on brain structural integrity.

Combined with MRI, molecular imaging may help identify neuroendocrine-driven events leading to a concomitant modulation in SWA and myelin. It would for example be interesting to assess the role of potential mediators, such as gamma-Aminobutyric acid (GABA), the main inhibitory neurotransmitter in the central nervous system, glutamate dynamics or growth hormone secretion which are closely related to both sleep regulation and myelin formation (Gottesmann, 2002b; Lopez et al., 2019; Serrano-Regal et al., 2020; Spiegel et al., 2000; Turan et al., 2021).

As a main outcome of our analysis, we used normalized $SWA_{0–2h}$ over other frequency bands which is less prone to general EEG amplitude effects and allows for a more frequency-specific interpretation compared to absolute levels. Intriguingly, when repeating the analysis using absolute $SWA_{0–2h}$, no significant association was observed for any MR-derived markers, suggesting that the power distribution across frequencies or more specifically the prevalence of power in the slow oscillatory range is also of relevance when probing for selective sleep-related correlates of brain structure.

Finally, a full topographical approach to assess spatial SWA distribution by using high-density EEG and a more in-depth characterization of SW characteristics, including slope and amplitude reflects exciting future research avenues to further explore the association between local SWA and regional myelin integrity.

6. Conclusion

Our results suggest that interindividual differences in the expression of sleep slow-wave activity, rather than its state-dependent intra-individual homeostatic dynamics or its frontal to occipital predominance, are associated with gray and white myelin estimates during early adulthood. During this stage of life, age-related frontal SWA decline seems to rather specifically echo ongoing myelination in late developing temporal portion of the ILF. Our results should be interpreted in a framework of continued post-adolescence brain development where myelination is ongoing in a region-specific manner and temporally matches changes in SWA dynamics.

Declaration of Competing Interest

The authors declare no competing interest.

Data Availability

Anonymized data created for the study are or will be available in a persistent repository upon publication, including processed MRI images, summary statistics of EEG data and demographic information. Codes and scripts used to process the data will be available in the same repository (DOI/ accession number: 10.5281/zenodo.6546548).

Acknowledgments

M.D., M.B., C.S., F.C., C.P., and G.V. are supported by the Fonds National de la Recherche Scientifique-FNRS-Belgium (F.R.S.-FNRS). M.B., M.R., G.H. and V.M. are supported by the European Research

Council (COGNAP-GA-757763). D.J.D. is supported by the UK Dementia Research Institute (DRI). S.L.C. is supported by the Alexander Von Humboldt Foundation. M.V.E. is supported by BrightFocus Foundation (A20211016F). The study was supported by the Wallonia-Brussels Federation (Actions de Recherche Concertées-ARC-09/14-03), WELBIO/Walloon Excellence in Life Sciences and Biotechnology Grant (WELBIO-CR-2010-06E), FNRS-Belgium (F.R.S-FNRS - F.4513.17 & T.0242.19 & 3.4516.11), Fondation Recherche Alzheimer (SAO-FRA 2019/0025), University of Liège (ULiège), Fondation Simone et Pierre Clerdent, European Regional Development Fund (Radiomed project), Fonds Léon Fredericq. D.J.D. is supported by the UK Dementia Research Institute (DRI). S.L.C. is supported by the Alexander Von Humboldt Foundation. M.B., M.R., G.H. and V.M. are supported by the European Research Council (COGNAP-GA-757763). M.V.E. is supported by BrightFocus Foundation (A20211016F). DJDC. is supported by the Alexander Von Humboldt Foundation. M.R., G.H. and V.M. are supported by the European Research Council (COGNAP-GA-757763). M.V.E. is supported by BrightFocus Foundation (A20211016F).

Supplementary materials

Supplementary material associated with this article can be found, in the online version, at doi:10.1016/j.neuroimage.2023.120045.

References

Achermann, P., Borbély, A.A., 2003. Mathematical models of sleep regulation. Front. Biosci.-Landmark 8, 683–693. doi:10.2741/1064.

Achermann, P., Borbély, A.A., 1990. Simulation of human sleep: ultradian dynamics of electroencephalographic slow-wave activity. J. Biol. Rhythms 5, 141–157. doi:10.1177/074873049000500206.

Åkerstedt, T., Gillberg, M., 1990. Subjective and objective sleepiness in the active individual. Int. J. Neurosci. 52, 29–37. doi:10.3109/00207459008994241.

Armstrong, C.L., Traipe, E., Hunter, J.V., Haselgrove, J.C., Ledakis, G.E., Tallent, E.M., Shera, D., Van Buchem, M.A., 2004. Age-related, regional, hemispheric, and medial-lateral differences in myelin integrity in vivo in the normal adult brain. AJNR Am. J. Neuroradiol. 25, 977.

Ashburner, J., 2007. A fast diffeomorphic image registration algorithm. Neuroimage 38, 95–113. doi:10.1016/j.neuroimage.2007.07.007.

Bartzokis, G., Beckson, M., Lu, P.H., Nuechterlein, K.H., Edwards, N., Mintz, J., 2001. Age-related changes in frontal and temporal lobe volumes in men: a magnetic resonance imaging study. Arch. Gen. Psychiatry 58, 461–465. doi:10.1001/archpsyc.58.5.461.

Bartzokis, G., Lu, P.H., Tingus, K., Mendez, M.F., Richard, A., Peters, D.G., Oluwadara, B., Barrall, K.A., Finn, J.P., Villablanca, P., Thompson, P.M., Mintz, J., 2010. Lifespan trajectory of myelin integrity and maximum motor speed. Neurobiol. Aging 31, 1554–1562. doi:10.1016/j.neurobiolaging.2008.08.015.

Bechler, M.E., Swire, M., ffrench-Constant, C., 2018. Intrinsic and adaptive myelination—a sequential mechanism for smart wiring in the brain. Dev. Neurobiol. 78, 68–79. doi:10.1002/dneu.22518.

Beck, A.T., Steer, R.A., Carbin, M.G., 1988. Psychometric properties of the Beck Depression Inventory: twenty-five years of evaluation. Clin. Psychol. Rev. 8, 77–100. doi:10.1016/0272-7358(88)90050-5.

Bellesi, M., Pfister-Genskow, M., Maret, S., Keles, S., Tononi, G., Cirelli, C., 2013. Effects of sleep and wake on oligodendrocytes and their precursors. J. Neurosci. 33, 14288–14300. doi:10.1523/JNEUROSCI.5102-12.2013.

Berthomier, C., Muto, V., Schmidt, C., Vandewalle, G., Jaspar, M., Devillers, J., Gaggioni, G., Chellappa, S.L., Meyer, C., Phillips, C., Salmon, E., Berthomier, P., Prado, J., Benoit, O., Bouet, R., Brandewinder, M., Mattout, J., Maquet, P., 2020. Exploring scoring methods for research studies: accuracy and variability of visual and automated sleep scoring. J. Sleep Res. 29. doi:10.1111/jsr.12994.

Bethlehem, R.A.I., Seidlitz, J., White, S.R., Vogel, J.W., Anderson, K.M., Adamson, C., Adler, S., Alexopoulos, G.S., Anagnostou, E., Areces-Gonzalez, A., Astle, D.E., Auyeung, B., Ayub, M., Bae, J., Ball, G., Baron-Cohen, S., Beare, R., Bedford, S.A., Benegal, V., Beyer, F., Blangero, J., Blesa Cábez, M., Boardman, J.P., Borzage, M., Bosch-Bayard, J.F., Bourke, N., Calhoun, V.D., Chakravarty, M.M., Chen, C., Chertavian, C., Chetelat, G., Chong, Y.S., Cole, J.H., Corvin, A., Costantino, M., Courchesne, E., Crivello, F., Cropley, V.L., Crosbie, J., Crossley, N., Delarue, M., Delorme, R., Desrivieres, S., Devenyi, G.A., Di Biase, M.A., Dolan, R., Donald, K.A., Donohoe, G., Dunlop, K., Edwards, A.D., Elison, J.T., Ellis, C.T., Elman, J.A., Eyler, L., Fair, D.A., Feczko, E., Fletcher, P.C., Fonagy, P., Franz, C.E., Galan-Garcia, L., Gholipour, A., Giedd, J., Gilmore, J.H., Glahn, D.C., Goodyer, I.M., Grant, P.E., Groenewold, N.A., Gunning, F.M., Gur, R.E., Gur, R.C., Hammill, C.F., Hansson, O., Hedden, T., Heinz, A., Henson, R.N., Heuer, K., Hoare, J., Holla, B., Holmes, A.J., Holt, R., Huang, H., Im, K., Ipser, J., Jack, C.R., Jackowski, A.P., Jia, T., Johnson, K.A., Jones, P.B., Jones, D.T., Kahn, R.S., Karlsson, H., Karlsson, L., Kawashima, R., Kelley, E.A., Kern, S., Kim, K.W., Kitzbichler, M.G., Kremen, W.S., Lalonde, F., Landeau, B., Lee, S., Lerch, J., Lewis, J.D., Li, J., Liao, W., Liston, C., Lombardo, M.V., Lv, J., Lynch, C., Mallard, T.T., Marcelis, M., Markello, R.D., Mathias, S.R., Mazoyer, B., McGuire, P., Meaney, M.J., Mechelli, A., Medic, N., Misic, B., Morgan, S.E., Mothersill, D., Nigg, J., Ong, M.Q.W., Ortinau, C., Ossenkoppele, R., Ouyang, M., Palaniyappan, L., Paly, L., Pan, P.M., Pantelis, C., Park, M.M., Paus, T., Pausova, Z., Paz-Linares, D., Pichet Binette, A., Pierce, K., Qian, X., Qiu, J., Qiu, A., Raznahan, A., Rittman, T., Rodrigue, A., Rollins, C.K., Romero-Garcia, R., Ronan, L., Rosenberg, M.D., Rowitch, D.H., Salum, G.A., Satterthwaite, T.D., Schaare, H.L., Schachar, R.J., Schultz, A.P., Schumann, G., Schöll, M., Sharp, D., Shinohara, R.T., Skoog, I., Smyser, C.D., Sperling, R.A., Stein, D.J., Stolicyn, A., Suckling, J., Sullivan, G., Taki, Y., Thyreau, B., Toro, R., Traut, N., Tsvetanov, K.A., Turk-Browne, N.B., Tuulari, J.J., Tzourio, C., Vachon-Presseau, É., Valdes-Sosa, M.J., Valdes-Sosa, P.A., Valk, S.L., van Amelsvoort, T., Vandekar, S.N., Vasung, L., Victoria, L.W., Villeneuve, S., Villringer, A., Vértes, P.E., Wagstyl, K., Wang, Y.S., Warfield, S.K., Warrier, V., Westman, E., Westwater, M.L., Whalley, H.C., Witte, A.V., Yang, N., Yeo, B., Yun, H., Zalesky, A., Zar, H.J., Zettergren, A., Zhou, J.H., Ziauddeen, H., Zugman, A., Zuo, X.N., 3R-BRAIN, AIBL, Alzheimer's Disease Neuroimaging Initiative, Alzheimer's Disease Repository Without Borders Investigators, CALM Team, Cam-CAN, CCNP, COBRE, CVEDA, ENIGMA Developmental Brain Age Working Group, Developing Human Connectome Project, FinnBrain, Harvard Aging Brain Study, IMAGEN, KNE96, Mayo Clinic Study of Aging, NSPN, POND, PREVENT-AD Research Group, VETSA, Bullmore, E.T., Alexander-Bloch, A.F., 2022. Brain charts for the human lifespan. Nature 604, 525–533. doi:10.1038/S41586-022-04554-Y.

Borbély, A.A., 1982. A two process model of sleep regulation. Hum. Neurobiol. 1, 195–204.

Borbely, A.A., Achermann, P., 1999. Sleep homeostasis and models of sleep regulation. J. Biol. Rhythms 14, 559–570. doi:10.1177/074873099129000894.

Buchmann, A., Kurth, S., Ringli, M., Geiger, A., Jenni, O.G., Huber, R., 2011. Anatomical markers of sleep slow wave activity derived from structural magnetic resonance images. J. Sleep Res. 20, 506–513. doi:10.1111/J.1365-2869.2011.00916.X.

Buysse, D.J., Reynolds, C.F., Monk, T.H., Berman, S.R., Kupfer, D.J., 1989. The Pittsburgh sleep quality index: a new instrument for psychiatric practice and research. Psychiatry Res doi:10.1016/0165-1781(89)90047-4.

Cajochen, C., Foy, R., Dijk, D.J., 1999a. Frontal predominance of a relative increase in sleep delta and theta EEG activity after sleep loss in humans. Sleep Res. Online SRO 2, 65–69.

Cajochen, C., Khalsa, S.B., Wyatt, J.K., Czeisler, C.A., Dijk, D.J., 1999b. EEG and ocular correlates of circadian melatonin phase and human performance decrements during sleep loss. Am. J. Physiol. 277, R640–R649. doi:10.1152/ajpregu.1999.277.3.r640.

Callaghan, M.F., Freund, P., Draganski, B., Anderson, E., Cappelletti, M., Chowdhury, R., Diedrichsen, J., FitzGerald, T.H.B., Smittenaar, P., Helms, G., Lutti, A., Weiskopf, N., 2014. Widespread age-related differences in the human brain microstructure revealed by quantitative magnetic resonance imaging. Neurobiol. Aging 35, 1862–1872. doi:10.1016/j.neurobiolaging.2014.02.008.

Campbell, J.S.W., Leppert, I.R., Narayanan, S., Boudreau, M., Duval, T., Cohen-Adad, J., Pike, G.B., Stikov, N., 2018. Promise and pitfalls of g-ratio estimation with MRI. NeuroImage, Microstruct. Imaging 182, 80–96. doi:10.1016/j.neuroimage.2017.08.038.

Carrier, J., Land, S., Buysse, D.J., Kupfer, D.J., Monk, T.H., 2001. The effects of age and gender on sleep EEG power spectral density in the middle years of life (ages 20–60 years old). Psychophysiology 38, 232–242. doi:10.1111/1469-8986.3820232.

Castaldi, E., Lunghi, C., Morrone, M.C., 2020. Neuroplasticity in adult human visual cortex. Neurosci. Biobehav. Rev. 112, 542–552. doi:10.1016/j.neubiorev.2020.02.028.

Corrigan, N.M., Yarnykh, V.L., Hippe, D.S., Owen, J.P., Huber, E., Zhao, T.C., Kuhl, P.K., 2021. Myelin development in cerebral gray and white matter during adolescence and late childhood. Neuroimage 227, 117678. doi:10.1016/j.neuroimage.2020.117678.

de Vivo, L., Bellesi, M., 2019. The role of sleep and wakefulness in myelin plasticity. Glia doi:10.1002/glia.23667.

Deoni, S.C.L., Mercure, E., Blasi, A., Gasston, D., Thomson, A., Johnson, M., Williams, S.C.R., Murphy, D.G.M., 2011. Mapping infant brain myelination with magnetic resonance imaging. J. Neurosci. 31, 784–791. doi:10.1523/JNEUROSCI.2106-10.2011.

Dijk, D.-J., 2009. Regulation and functional correlates of slow wave sleep. J. Clin. Sleep Med. JCSM Off. Publ. Am. Acad. Sleep Med. 5, S6–S15.

Dijk, D.J., 2006. Sleep of aging women and men: back to basics. Sleep 29, 12–13. doi:10.1093/SLEEP/29.1.12.

Dijk, D.J., Beersma, D.G.M., Bloem, G.M., 1989. Sex differences in the sleep EEG of young adults: visual scoring and spectral analysis. Sleep 12, 500–507. doi:10.1093/SLEEP/12.6.500.

Dijk, D.J., Beersma, D.G.M., Daan, S., 1987. EEG power density during nap sleep: reflection of an hourglass measuring the duration of prior wakefulness. J. Biol. Rhythms 2, 207–219. doi:10.1177/074873048700200304.

Dijk, D.J., Brunner, D.P., Borbely, A.A., 1990. Time course of EEG power density during long sleep in humans. Am. J. Physiol. - Regul. Integr. Comp. Physiol. 258. doi:10.1152/ajpregu.1990.258.3.r650.

Dijk, D.J., Czeisler, C.A., 1995. Contribution of the circadian pacemaker and the sleep homeostat to sleep propensity, sleep structure, electroencephalographic slow waves, and sleep spindle activity in humans. J. Neurosci. 15, 3526–3538. doi:10.1523/jneurosci.15-05-03526.1995.

Dinges, D.F., Powell, J.W., 1985. Microcomputer analyses of performance on a portable, simple visual RT task during sustained operations. Behav. Res. Methods Instrum. Comput. 17, 652–655. doi:10.3758/BF03200977.

Draganski, B., Ashburner, J., Hutton, C., Kherif, F., Frackowiak, R.S.J., Helms, G., Weiskopf, N., 2011. Regional specificity of MRI contrast parameter changes in normal ageing revealed by voxel-based quantification (VBQ). Neuroimage 55, 1423–1434. doi:10.1016/j.neuroimage.2011.01.052.

Dubè, J., Lafortune, M., Bedetti, C., Bouchard, M., Gagnon, J.F., Doyon, J., Evans, A.C., Lina, J.M., Carrier, J., 2015. Cortical thinning explains changes in sleep slow waves during adulthood. J. Neurosci. 35, 7795–7807. doi:10.1523/JNEUROSCI.3956-14.2015.

Farokhian, F., Beheshti, I., Sone, D., Matsuda, H., 2017. Comparing CAT12 and VBM8 for detecting brain morphological abnormalities in temporal lobe epilepsy. Front. Neurol. 8. doi:10.3389/fneur.2017.00428.

Finelli, L.A., Borbély, A.A., Achermann, P., 2001. Functional topography of the human nonREM sleep electroencephalogram. Eur. J. Neurosci. 13, 2282–2290. doi:10.1046/J.0953-816X.2001.01597.X.

Franken, P., Chollet, D., Tafti, M., 2001. The homeostatic regulation of sleep need is under genetic control. J. Neurosci. 21, 2610–2621. doi:10.1523/jneurosci.21-08-02610.2001.

Frazier, J.A., Chiu, S., Breeze, J.L., Makris, N., Lange, N., Kennedy, D.N., Herbert, M.R., Bent, E.K., Koneru, V.K., Dieterich, M.E., Hodge, S.M., Rauch, S.L., Grant, P.E., Cohen, B.M., Seidman, L.J., Caviness, V.S., Biederman, J., 2005. Structural brain magnetic resonance imaging of limbic and thalamic volumes in pediatric bipolar disorder. Am. J. Psychiatry 162, 1256–1265. doi:10.1176/appi.ajp.162.7.1256.

Gaser, C., Dahnke, R., 2016. CAT-a computational anatomy toolbox for the analysis of structural MRI data. Hbm 2016, 336–348.

Gaudreau, H., Carrier, J., Montplaisir, J., 2001. Age-related modifications of NREM sleep EEG: from childhood to middle age. J. Sleep Res. 10, 165–172. doi:10.1046/j.1365-2869.2001.00252.x.

Giorgio, A., Watkins, K.E., Chadwick, M., James, S., Winmill, L., Douaud, G., De Stefano, N., Matthews, P.M., Smith, S.M., Johansen-Berg, H., James, A.C., 2010. Longitudinal changes in grey and white matter during adolescence. Neuroimage 49, 94–103. doi:10.1016/j.neuroimage.2009.08.003.

Gogtay, N., Thompson, P.M., 2010. Mapping gray matter development: implications for typical development and vulnerability to psychopathology. Brain Cogn doi:10.1016/j.bandc.2009.08.009.

Gottesmann, C., 2002. GABA mechanisms and sleep. Neuroscience doi:10.1016/S0306-4522(02)00034-9.

Grumbach, P., Opel, N., Martin, S., Meinert, S., Leehr, E.J., Redlich, R., Enneking, V., Goltermann, J., Baune, B.T., Dannlowski, U., Repple, J., 2020. Sleep duration is associated with white matter microstructure and cognitive performance in healthy adults. Hum. Brain Mapp. 41, 4397–4405. doi:10.1002/hbm.25132.

Hagiwara, A., Hori, M., Kamagata, K., Warntjes, M., Matsuyoshi, D., Nakazawa, M., Ueda, R., Andica, C., Koshino, S., Maekawa, T., Irie, R., Takamura, T., Kumamaru, K.K., Abe, O., Aoki, S., 2018. Myelin measurement: comparison between simultaneous tissue relaxometry, magnetization transfer saturation index, and T1w/T2w ratio. Methods. Sci. Rep. 8, 10554. doi:10.1038/s41598-018-28852-6.

Helms, G., Weiskopf, N., Lutti, A., 2021. Correction of FLASH-based MT saturation in human brain for residual bias of B1-inhomogeneity at 3T.

Horne, J.A., Ostberg, O., 1976. A self-assessment questionnaire to determine morningness-eveningness in human circadian rhythms. Int. J. Chronobiol. doi:10.1177/0748730405285278.

Iber, C., Ancoli-Israel, S., Chesson, A.L., Quan, S.F., 2007. The new sleep scoring manual - the evidence behind the rules. J. Clin. Sleep Med. doi:10.5664/jcsm.26812.

John Raven, J., 2003. Raven Progressive Matrices, in: Handbook of Nonverbal Assessment. Springer, Boston, MA, pp. 223–237. doi:10.1007/978-1-4615-0153-4_11.

Khalsa, S., Hale, J.R., Goldstone, A., Wilson, R.S., Mayhew, S.D., Bagary, M., Bagshaw, A.P., 2017. Habitual sleep durations and subjective sleep quality predict white matter differences in the human brain. Neurobiol. Sleep Circadian Rhythms 3, 17–25. doi:10.1016/j.nbscr.2017.03.001.

Kirchner, W.K., 1958. Age differences in short-term retention of rapidly changing information. J. Exp. Psychol. 55, 352–358. doi:10.1037/h0043688.

Kurth, S., Jenni, O.G., Riedner, B.A., Tononi, G., Carskadon, M.A., Huber, R., 2010a. Characteristics of sleep slow waves in children and adolescents. Sleep 33, 475–480. doi:10.1093/sleep/33.4.475.

Kurth, S., Riedner, B.A., Dean, D.C., O'Muircheartaigh, J., Huber, R., Jenni, O.G., Deoni, S.C.L., LeBourgeois, M.K., 2017. Traveling slow oscillations during sleep: a marker of brain connectivity in childhood. Sleep 40. doi:10.1093/sleep/zsx121, zsx121.

Kurth, S., Ringli, M., Geiger, A., LeBourgeois, M., Jenni, O.G., Huber, R., 2010b. Mapping of cortical activity in the first two decades of life: a high-density sleep electroencephalogram study. J. Neurosci. 30, 13211–13219. doi:10.1523/JNEUROSCI.2532-10.2010.

Lazar, A.S., Lazar, Z.I., Dijk, D.-J., 2015. Circadian regulation of slow waves in human sleep: topographical aspects. Neuroimage 116, 123–134. doi:10.1016/j.neuroimage.2015.05.012.

LeBourgeois, M.K., Dean, D.C., Deoni, S.C.L., Kohler, M., Kurth, S., 2019. A simple sleep EEG marker in childhood predicts brain myelin 3.5 years later. Neuroimage 199, 342–350. doi:10.1016/j.neuroimage.2019.05.072.

Ling, C.L., Rumpel, H., 2006. MRI atlas of human white matter. Concepts Magn. Reson. Part A 28A 181–182. doi:10.1002/cmr.a.20052.

Lopez, J., Quan, A., Budihardjo, J., Xiang, S., Wang, H., Koshy, Kiron, Cashman, C., Lee, W.P.A., Hoke, A., Tuffaha, S., Brandacher, G., 2019. Growth hormone improves nerve regeneration, muscle Re-innervation, and functional outcomes after chronic denervation injury. Sci. Rep. 9, 3117. doi:10.1038/s41598-019-39738-6.

Lutti, A., Stadler, J., Josephs, O., Windischberger, C., Speck, O., Bernarding, J., Hutton, C., Weiskopf, N., 2012. Robust and fast whole brain mapping of the RF transmit field B1 at 7T. PLoS ONE 7. doi:10.1371/journal.pone.0032379.

Lynch, K.M., Cabeen, R.P., Toga, A.W., Clark, K.A., 2020. Magnitude and timing of major white matter tract maturation from infancy through adolescence with NODDI. Neuroimage 212, 116672. doi:10.1016/j.neuroimage.2020.116672.

Mehta, R.C., Pike, G.B., Enzmann, D.R., 1995. Magnetization transfer MR of the normal adult brain. AJNR Am. J. Neuroradiol. 16, 2085.

Miller, D.J., Duka, T., Stimpson, C.D., Schapiro, S.J., Baze, W.B., McArthur, M.J., Fobbs, A.J., Sousa, A.M.M., Sěstan, N., Wildman, D.E., Lipovich, L., Kuzawa, C.W., Hof, P.R., Sherwood, C.C., 2012. Prolonged myelination in human neocortical evolution. Proc. Natl. Acad. Sci. U. S. A. 109, 16480–16485. doi:10.1073/pnas.1117943109.

Mulder, T.A., Kocevska, D., Muetzel, R.L., Koopman-Verhoeff, M.E., Hillegers, M.H., White, T., Tiemeier, H., 2019. Childhood sleep disturbances and white matter microstructure in preadolescence. J. Child Psychol. Psychiatry 60, 1242–1250. doi:10.1111/jcpp.13085.

Muto, V., Koshmanova, E., Ghaemmaghami, P., Jaspar, M., Meyer, C., Elansary, M., Van Egroo, M., Chylinski, D., Berthomier, C., Brandewinder, M., Mouraux, C., Schmidt, C., Hammad, G., Coppieters, W., Ahariz, N., Degueldre, C., Luxen, A., Salmon, E., Phillips, C., Archer, S.N., Yengo, L., Byrne, E., Collette, F., Georges, M., Dijk, D.J., Maquet, P., Visscher, P.M., Vandewalle, G., 2021. Alzheimer's disease genetic risk and sleep phenotypes in healthy young men: association with more slow waves and daytime sleepiness. Sleep 44. doi:10.1093/sleep/zsaa137.

Ohki, T., Gunji, A., Takei, Y., Takahashi, H., Kaneko, Y., Kita, Y., Hironaga, N., Tobimatsu, S., Kamio, Y., Hanakawa, T., Inagaki, M., Hiraki, K., 2016. Neural oscillations in the temporal pole for a temporally congruent audio-visual speech detection task. Sci. Rep. 6, 37973. doi:10.1038/srep37973.

Ohtsuki, G., Shishikura, M., Ozaki, A., 2020. Synergistic excitability plasticity in cerebellar functioning. FEBS J 287, 4557–4593. doi:10.1111/febs.15355.

Paus, T., 2005. Mapping brain maturation and cognitive development during adolescence. Trends Cogn. Sci. doi:10.1016/j.tics.2004.12.008.

Petanjek, Z., Judaš, M., Šimić, G., Rašin, M.R., Uylings, H.B.M., Rakic, P., Kostović, I., 2011. Extraordinary neoteny of synaptic spines in the human prefrontal cortex. Proc. Natl. Acad. Sci 108, 13281–13286. doi:10.1073/pnas.1105108108.

Piantoni, G., Poil, S.S., Linkenkaer-Hansen, K., Verweij, I.M., Ramautar, J.R., Van Someren, E.J.W., Van Der Werf, Y.D., 2013a. Individual differences in white matter diffusion affect sleep oscillations. J. Neurosci. 33, 227–233. doi:10.1523/JNEUROSCI.2030-12.2013.

Piantoni, G., Poil, S.S., Linkenkaer-Hansen, K., Verweij, I.M., Ramautar, J.R., Van Someren, E.J.W., Van Der Werf, Y.D., 2013b. Individual differences in white matter diffusion affect sleep oscillations. J. Neurosci. 33, 227–233. doi:10.1523/JNEUROSCI.2030-12.2013.

Robertson, I.H., Manly, T., Andrade, J., Baddeley, B.T., Yiend, J., 1997. Oops!": performance correlates of everyday attentional failures in traumatic brain injured and normal subjects. Neuropsychologia 35, 747–758. doi:10.1016/s0028-3932(97)00015-8.

Rusterholz, T., Tarokh, L., Van Dongen, H.P.A., Achermann, P., 2017. Interindividual differences in the dynamics of the homeostatic process are trait-like and distinct for sleep versus wakefulness. J. Sleep Res. 26, 171–178. doi:10.1111/jsr.12483.

Sanchez, E., El-Khatib, H., Arbour, C., Bedetti, C., Blais, H., Marcotte, K., Baril, A.A., Descoteaux, M., Gilbert, D., Carrier, J., Gosselin, N., 2019. Brain white matter damage and its association with neuronal synchrony during sleep. Brain 142, 674–687. doi:10.1093/BRAIN/AWY348.

Schmierer, K., Scaravilli, F., Altmann, D.R., Barker, G.J., Miller, D.H., 2004. Magnetization transfer ratio and myelin in postmortem multiple sclerosis brain. Ann. Neurol. 56, 407–415. doi:10.1002/ana.20202.

Seabold, S., Perktold, J., 2010. Statsmodels: econometric and Statistical Modeling with Python. In: Proceedings of the 9th Python in Science Conference, pp. 92–96. doi:10.25080/majora-92bf1922-011.

Serrano-Regal, M.P., Luengas-Escuza, I., Bayón-Cordero, L., Ibarra-Aizpurua, N., Alberdi, E., Pérez-Samartín, A., Matute, C., Sánchez-Gómez, M.V., 2020. Oligodendrocyte differentiation and myelination is potentiated via GABAB receptor activation. Neuroscience 439, 163–180. doi:10.1016/j.neuroscience.2019.07.014.

Shaw, P., Kabani, N.J., Lerch, J.P., Eckstrand, K., Lenroot, R., Gogtay, N., Greenstein, D., Clasen, L., Evans, A., Rapoport, J.L., Giedd, J.N., Wise, S.P., 2008. Neurodevelopmental trajectories of the human cerebral cortex. J. Neurosci. 28, 3586–3594. doi:10.1523/JNEUROSCI.5309-07.2008.

Song, S.K., Sun, S.W., Ramsbottom, M.J., Chang, C., Russell, J., Cross, A.H., 2002. Dysmyelination revealed through MRI as increased radial (but unchanged axial) diffusion of water. Neuroimage 17, 1429–1436. doi:10.1006/nimg.2002.1267.

Spiegel, K., Leproult, R., Colecchia, E.F., L'Hermite-Balériaux, M., Nie, Z., Copinschi, G., Van Cauter, E., 2000. Adaptation of the 24-h growth hormone profile to a state of sleep debt. Am. J. Physiol. Regul. Integr. Comp. Physiol. 279, R874–R883. doi:10.1152/ajpregu.2000.279.3.R874.

Swire, M., Ffrench-Constant, C., 2018. Seeing is believing: myelin dynamics in the adult CNS. Neuron doi:10.1016/j.neuron.2018.05.005.

Tabelow, K., Balteau, E., Ashburner, J., Callaghan, M.F., Draganski, B., Helms, G., Kherif, F., Leutritz, T., Lutti, A., Phillips, C., Reimer, E., Ruthotto, L., Seif, M., Weiskopf, N., Ziegler, G., Mohammadi, S., 2019. hMRI – a toolbox for quantitative MRI in neuroscience and clinical research. Neuroimage 194, 191–210. doi:10.1016/j.neuroimage.2019.01.029.

Tai, X.Y., Chen, C., Manohar, S., Husain, M., 2022. Impact of sleep duration on executive function and brain structure. Commun. Biol. 5, 1–10. doi:10.1038/s42003-022-03123-3.

Tarokh, L., Raffray, T., Van Reen, E., Carskadon, M.A., 2010. Physiology of normal sleep in adolescents. Adolesc. Med. State Art Rev. 21, 401–417 vii.

Terribilli, D., Schaufelberger, M.S., Duran, F.L.S., Zanetti, M.V., Curiati, P.K., Menezes, P.R., Scazufca, M., Amaro, E., Leite, C.C., Busatto, G.F., 2011. Age-related gray matter volume changes in the brain during non-elderly adulthood. Neurobiol. Aging 32, 354–368. doi:10.1016/j.neurobiolaging.2009.02.008.

Timmler, S., Simons, M., 2019. Grey matter myelination. Glia 67, 2063–2070. doi:10.1002/GLIA.23614.

Tononi, G., Cirelli, C., 2014. Sleep and the price of plasticity: from synaptic and cellular homeostasis to memory consolidation and integration. Neuron 81, 12–34. doi:10.1016/j.neuron.2013.12.025.

Turan, F., Yilmaz, Ö., Schünemann, L., Lindenberg, T.T., Kalanithy, J.C., Harder, A., Ahmadi, S., Duman, T., MacDonald, R.B., Winter, D., Liu, C., Odermatt, B., 2021. Effect of modulating glutamate signaling on myelinating oligodendrocytes and their development—A study in the zebrafish model. J. Neurosci. Res. 99, 2774–2792. doi:10.1002/jnr.24940.

Turati, L., Moscatelli, M., Mastropietro, A., Dowell, N.G., Zucca, I., Erbetta, A., Cordiglieri, C., Brenna, G., Bianchi, B., Mantegazza, R., Cercignani, M., Baggi, F., Minati, L., 2015. In vivo quantitative magnetization transfer imaging correlates with histology during de- and remyelination in cuprizone-treated mice. NMR Biomed. 28, 327–337. doi:10.1002/nbm.3253.

Valk, S.L., Bernhardt, B.C., Trautwein, F.-.M., Böckler, A., Kanske, P., Guizard, N., Collins, D.L., Singer, T., 2017. Structural plasticity of the social brain: differential change after socio-affective and cognitive mental training. Sci. Adv. 3, e1700489. doi:10.1126/sciadv.1700489.

Voldsbekk, I., Groote, I., Zak, N., Roelfs, D., Geier, O., Due-Tønnessen, P., Løkken, L.L., Strømstad, M., Blakstvedt, T.Y., Kuiper, Y.S., Elvsåshagen, T., Westlye, L.T., Bjørnerud, A., Maximov, I.I., 2021. Sleep and sleep deprivation differentially alter white matter microstructure: a mixed model design utilising advanced diffusion modelling. Neuroimage 226. doi:10.1016/j.neuroimage.2020.117540.

Volk, C., Jaramillo, V., Merki, R., O'Gorman Tuura, R., Huber, R., 2018. Diurnal changes in glutamate + glutamine levels of healthy young adults assessed by proton magnetic resonance spectroscopy. Hum. Brain Mapp 39, 3984–3992. doi:10.1002/hbm.24225.

Vyazovskiy, V.V., Riedner, B.A., Cirelli, C., Tononi, G., 2007. Sleep homeostasis and cortical synchronization: II. A local field potential study of sleep slow waves in the rat. Sleep 30, 1631–1642.

Walker, M.P., 2021. Sleep essentialism. Brain 144, 697–699. doi:10.1093/brain/awab026.

Weiskopf, N., Edwards, L.J., Helms, G., Mohammadi, S., Kirilina, E., 2021. Quantitative magnetic resonance imaging of brain anatomy and in vivo histology. Nat. Rev. Phys. 38 (3), 570–588. doi:10.1038/s42254-021-00326-1, 2021.

Weiskopf, N., Suckling, J., Williams, G., Correia, M., MM, Inkster, B., Tait, R., Ooi, C., Bullmore, T.E.T., Lutti, A., 2013a. Quantitative multi-parameter mapping of R1, PD*, MT, and R2* at 3T: a multi-center validation. Front. Neurosci. 0, 95. doi:10.3389/fnins.2013.00095.

Weiskopf, N., Suckling, J., Williams, G., Correia, M., MM, Inkster, B., Tait, R., Ooi, C., Bullmore, T.E.T., Lutti, A., 2013b. Quantitative multi-parameter mapping of R1, PD*, MT, and R2* at 3T: a multi-center validation. Front. Neurosci. 7. doi:10.3389/fnins.2013.00095.

Werth, E., Dijk, D.J., Achermann, P., Borbély, A.A., 1996. Dynamics of the sleep EEG after an early evening nap: experimental data and simulations. Am. J. Physiol. 271. doi:10.1152/AJPREGU.1996.271.3.R501.

Yarnykh, V.L., 2007. Actual flip-angle imaging in the pulsed steady state: a method for rapid three-dimensional mapping of the transmitted radiofrequency field. Magn. Reson. Med. 57, 192–200. doi:10.1002/mrm.21120.